Optical Engineering

OpticalEngineering.SPIEDigitalLibrary.org

All-optical broadcast technology based on aluminum-doped highly nonlinear fiber

Lijuan Li
Jinlong Yu
Ju Wang
Wenrui Wang
Shi Jia
Qiong Wu
Lixia Dou
Biao Huang

SPIE.

All-optical broadcast technology based on aluminum-doped highly nonlinear fiber

Lijuan Li, Jinlong Yu, Ju Wang,* Wenrui Wang, Shi Jia, Qiong Wu, Lixia Dou, and Biao Huang
Tianjin University, School of Electrical and Information Engineering, Optical Fiber Communications Laboratory, Tianjin 300072, China

Abstract. Making use of the four-wave mixing, a realization of all-optical 1×6 broadcast technology based on aluminum-doped highly nonlinear fiber (AL-HNLF) is performed. In the system, a set of experiments at channel intervals of 50, 100, and 200 GHz are conducted, and clear eye diagrams as well as low error performance are obtained with an input optical signal of a continuous wave and a 10-Gb/s return-to-zero on-off keying signal, which mostly benefits from the AL-HNLF used in this system. In detail, resulting from the high stimulated Brillouin scattering threshold of AL-HNLF, more power can be launched into the fiber. Additionally, similar performances of different channel spaces demonstrate the adjustability for this technology. With these distinguishing features, this technology might satisfy the basic expectation of utility. [DOI: 10.1117/1.OE.53.11.116107]

Keywords: all-optical broadcast; aluminum-doped highly nonlinear fiber; four-wave mixing.

Paper 141131 received Jul. 16, 2014; revised manuscript received Oct. 13, 2014; accepted for publication Oct. 14, 2014; published online Nov. 11, 2014.

1 Introduction

Since optical fibers possess advantages such as transmission bandwidth, low transmission loss, anti-interference ability, and other characteristics, optical communication[1,2] technology has gained in popularity in the communications infrastructure. Optic-electric-optic (O/E/O) conversion is a result of its development. However, this existing (O/E/O) conversion is at the expense of a complex structure, high cost, and the highest conversion efficiency is limited to an "electronic bottleneck." Therefore, all-optical communication would be a more attractive strategy for communication modes. To be exact, the method of broadcast whose structure is simple as well as giving an advantage in terms of wavelength multiplexing tends to be more popular. [3,4]

The dominant implementations of all-optical broadcast are as follows: cross-gain modulation,[5–10] cross-phase modulation,[11–13] and four-wave mixing (FWM) for semiconductor optical amplifier (SOA)[14] and FWM for highly nonlinear fiber (HNLF).[15] Since FWM has the capability of signal processing transparently in data format[16] and can be used in both phase and intensity modulations, it attracts people's interest. Furthermore, compared with FWM for SOA, FWM for HNLF has a fast response, flat broadband, and low noise. However, stimulated Brillouin scattering (SBS)[17,18] limits the amount of power that can be launched into a fiber and the maximum nonlinearity that can be achieved from HNLF as well. Recently, a novel type of HNLF called aluminum-doped HNFL (AL-HNLF) has been of note for its SBS threshold, which is much higher than that of a conventional HNLF.[19] With a high SBS threshold, a more efficient nonlinear process can be obtained without SBS suppression. Interestingly, the experiments using AL-HNLF do result in a high performance. The bit error rates (BERs) of most data signals reach 10^{-9}, which indicates most signals are obtained with error-free performance. The BERs for the worst signals reach 10^{-3}, but their performance can still be improved by error correction.

In this paper, three similar experiments with channel intervals of 50, 100, and 200 GHz are conducted based on AL-HNLF and the results demonstrate a good performance of the broadcast technology based on AL-HNLF. Thus, it turns out to be adjustable and flexible for this technology in practical applications.

2 Principle of Broadcast

A 10-Gb/s return-to-zero signal (at the frequency of f_s) with a pump light (at the frequency of f_{cw}) is injected into the HNLF. As a result of the nonlinear effect in HNLF, two new signals that carry the broadcast information are generated and their frequencies are f_1 and f_2, respectively. The frequency relationships are given by

$$f_1 = 2f_s - f_{cw}, \tag{1}$$

$$f_2 = 2f_{cw} - f_s. \tag{2}$$

When the power of the two new signals is high enough to be a pump, another two new signals are produced at the frequencies of

$$f_3 = 2f_1 - f_2, \tag{3}$$

$$f_4 = 2f_2 - f_1. \tag{4}$$

Similarly, as long as the new signals meet the phase match condition and have enough power, higher-order signals will be generated. In other words, the information is copied in different wavelengths. Let c denote the velocity of the light in a vacuum. The FWM process in terms of wavelength could be derived by substituting $f = (c/\lambda)$ into Eqs. (1)–(4). Let us take Eq. (1) for example. The corresponding wavelength relationship is given by

*Address all correspondence to: Ju Wang, E-mail: wangju@tju.edu.cn

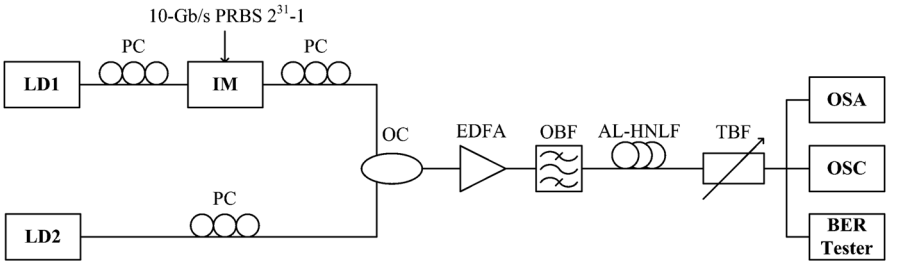

Fig. 1 Experimental system for aluminum-doped highly nonlinear fiber (AL-HNLF) based on broadcast of a 10-Gb/s return-to-zero signal.

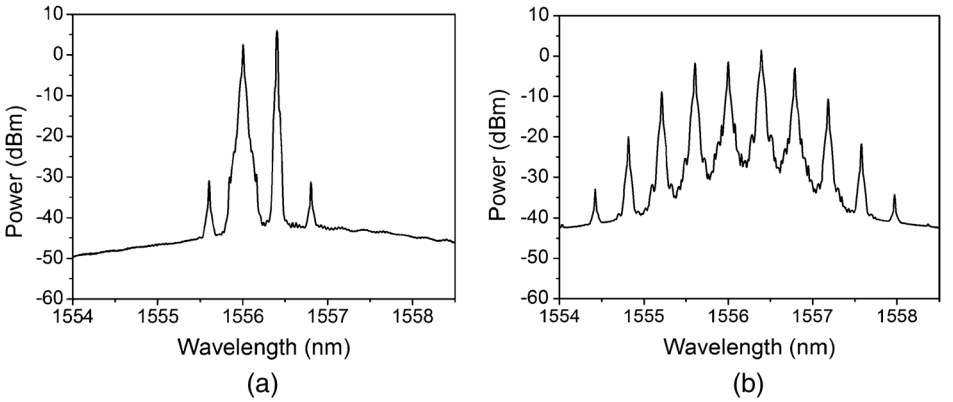

Fig. 2 Optical spectra at the (a) input and (b) output of the AL-HNLF with a channel interval of 50 GHz.

$$\frac{1}{\lambda_1}=\frac{2}{\lambda_s}-\frac{1}{\lambda_{cw}}, \tag{5}$$

$$\frac{\lambda_s-\lambda_1}{\lambda_1\lambda_s}=\frac{\lambda_{cw}-\lambda_s}{\lambda_{cw}\lambda_s}. \tag{6}$$

In our experiment, the slight wavelength differences among λ_{cw}, λ_s, λ_1 result in the approximate equation $(\lambda_1/\lambda_{cw})\approx 1$. Hence, Eq. (6) becomes

$$\lambda_1\approx 2\lambda_s-\lambda_{cw}. \tag{7}$$

The relationship in Eq. (7) works for Eqs. (2)–(4) and also works for the higher-order signals that are generated in the FWM process. In our experiments, we apply the approximate equations into the whole data analysis.

As shown in Fig. 1, the system components are the laser diode (LD), polarization controller (PC), intensity modulator (IM), erbium-doped fiber amplifier (EDFA), optical band-pass filter (OBF), 3-dB optical coupler (OC), AL-HNLF [length: 130 m, nonlinear coefficient: 7.4 $W^{-1}\,km^{-1}$, SBS threshold for 130 m: 1000 mW, attenuation: 15 dB/km, dispersion slope: $0.011 ps/(nm^2 km)$, effective area: $13.5\mu m^2$], tunable band-pass filter (TBF), oscilloscope (OSC), optical spectrum analyzer (OSA), and BER tester. LD1 generates a continuous wave (CW) at a wavelength of 1556 nm (λ_s), modulated by a 10-Gb/s pseudorandom bit sequence (2^{31}-1) electrical data signal. LD2 produces another CW (at the wavelength of λ_{cw}); for any CW, no additional SBS suppression stages are used in this system. We adjust the PC if necessary before they are coupled into the OC. At the input of EDFA, the average power is 1.1 dBm, and the coupled signal is amplified up to 34 dBm after the EDFA. Then the amplified signal passes through the 3-nm OBF to block amplified spontaneous emission noise, and is finally launched into AL-HNLF with an average input power of 33 dBm. Different wavelengths are filtered through the TBF, which are evaluated in the OSA. The corresponding eye diagrams are shown in the OSC. Meanwhile, a BER tester is applied to analyze the performances of broadcast signals.

3 Results

The performances for the configurations of a 50-GHz channel interval and 1556.4-nm wavelength of λ_{cw} generated by LD2 are described as follows.

Figure 2 depicts the optical spectra at the input and output of the AL-HNLF. As shown in Fig. 2(b), six new signals are detected. The wavelengths are 1555.6, 1556.8, 1555.2,

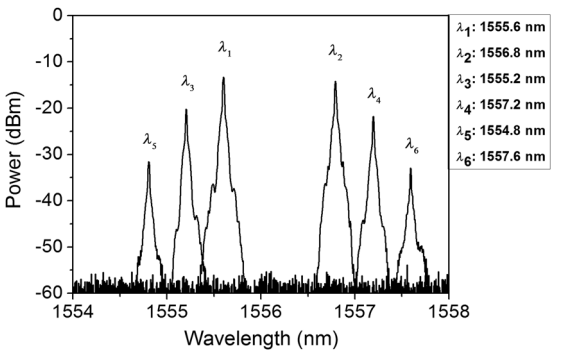

Fig. 3 Optical spectra of the broadcast signals after the filtering subsystem (channel space: 50 GHz).

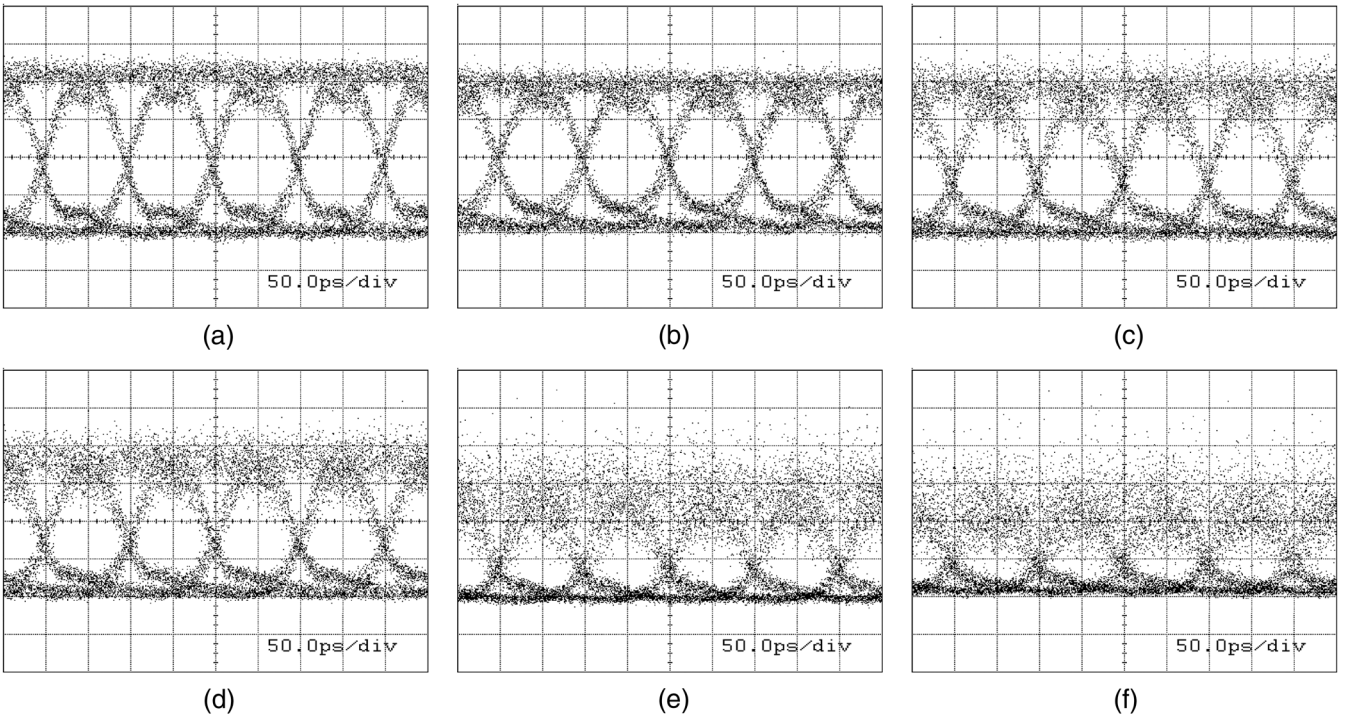

Fig. 4 Eye diagrams 1×6 broadcast at different wavelengths with channel interval of 50 GHz: (a) at 1555.6 nm (λ_1), (b) at 1556.8 nm (λ_2), (c) at 1555.2 nm (λ_3), (d) at 1557.2 nm (λ_4), (e) 1554.8 nm (λ_5), and (f) 1557.6 nm (λ_6).

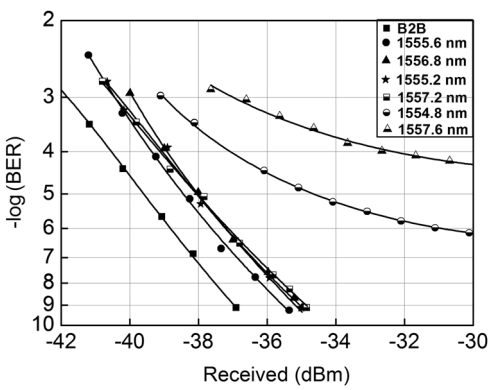

Fig. 5 BER curves of the six broadcast signals (channel space: 50 GHz).

1557.2, 1554.8, and 1557.6 nm, which are identical to the analysis above. Note that due to the device limit, before being fed into the AL-HNLF, the undesired frequency component could not be completely filtered out. Hence, as shown in Fig. 2(a), two remaining frequency components are found at λ_1 and λ_2, which are caused by the nonlinear process in the EDFA.

Figures 3 and 4 show the optical spectra and eye diagrams at different wavelengths of the new generated signals. With a decrease of power density from λ_1 to λ_6, the performance of the broadcast signals are deteriorated, especially at λ_5 (1554.8 nm) and λ_6 (1557.6 nm). Furthermore, the "0" level performs better than the "1" level. In brief, the clear eye diagrams from λ_1 to λ_4 demonstrate a good performance for the broadcast signals.

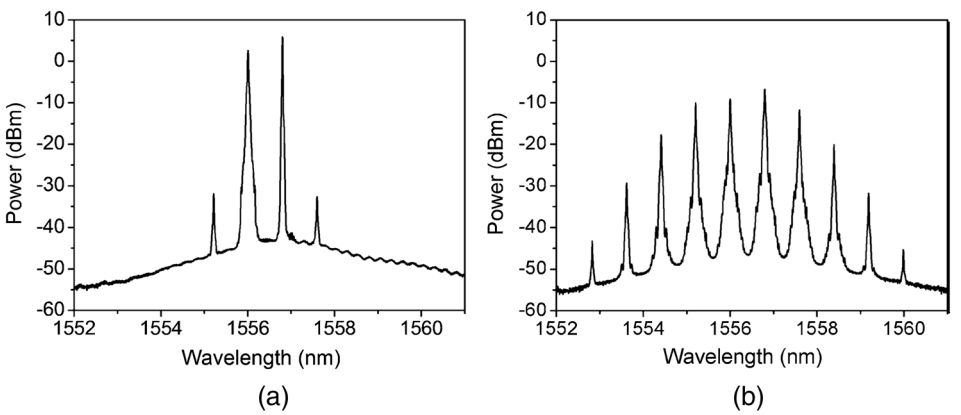

Fig. 6 Optical spectra at the (a) input and (b) output of the AL-HNLF with a channel interval of 100 GHz.

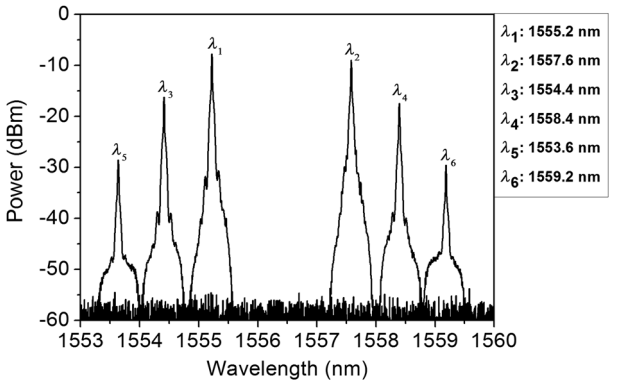

Fig. 7 Optical spectra of the broadcast signals after the filtering subsystem (channel space: 100 GHz).

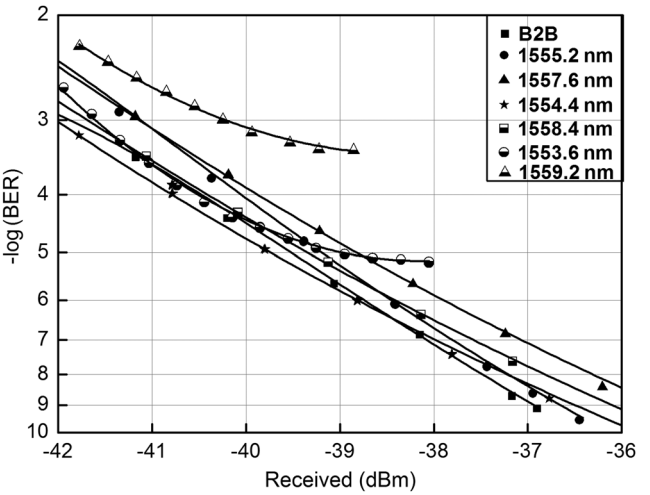

Fig. 9 BER curves of the six broadcast signals (channel space: 100 GHz).

The BERs of broadcast signals are shown in Fig. 5. Broadcast signals at λ_1 (1555.6 nm), λ_2 (1556.8 nm), λ_3 (1555.2 nm), and λ_4 (1557.2 nm) run error free with low power, while data signals at λ_5 (1554.8 nm) and λ_6 (1557.6 nm) require a relatively high power to offer an error-free (10^{-9}) approximation. However, an error floor (10^{-3}) exists for λ_5 (1554.8 nm) and λ_6 (1557.6 nm), which indicates that the performance of λ_5 (1554.8 nm) and λ_6 (1557.6 nm) could be improved with an error-correcting code stage.

The performances for the configurations of 100-GHz channel interval and 1556.8-nm wavelength of λ_{cw} generated by LD2 are described as follows.

Figure 6 represents the optical spectra at the input and output of the AL-HNLF. As shown in Fig. 6(b), six new signals are detected and their wavelengths are 1553.6, 1554.4, 1555.2, 1557.6, 1558.4, and 1559.2 nm. Figures 7 and 8 show the optical spectra and eye diagrams at different wavelengths for the new generated signals. The analysis is similar to 50 GHz. The BERs of the broadcast signals are shown in Fig. 9. The case is similar to 50 GHz.

The performances for the configurations of a 200-GHz channel interval and 1557.6-nm wavelength of λ_{cw} generated by LD2 are described as follows.

Figure 10 describes the optical spectra at the input and output of the AL-HNLF. As shown in Fig. 10(b), six new signals are detected and the wavelengths are 1554.4, 1559.2, 1552.8, 1560.8, 1551.2, and 1562.4 nm. Figures 11 and 12

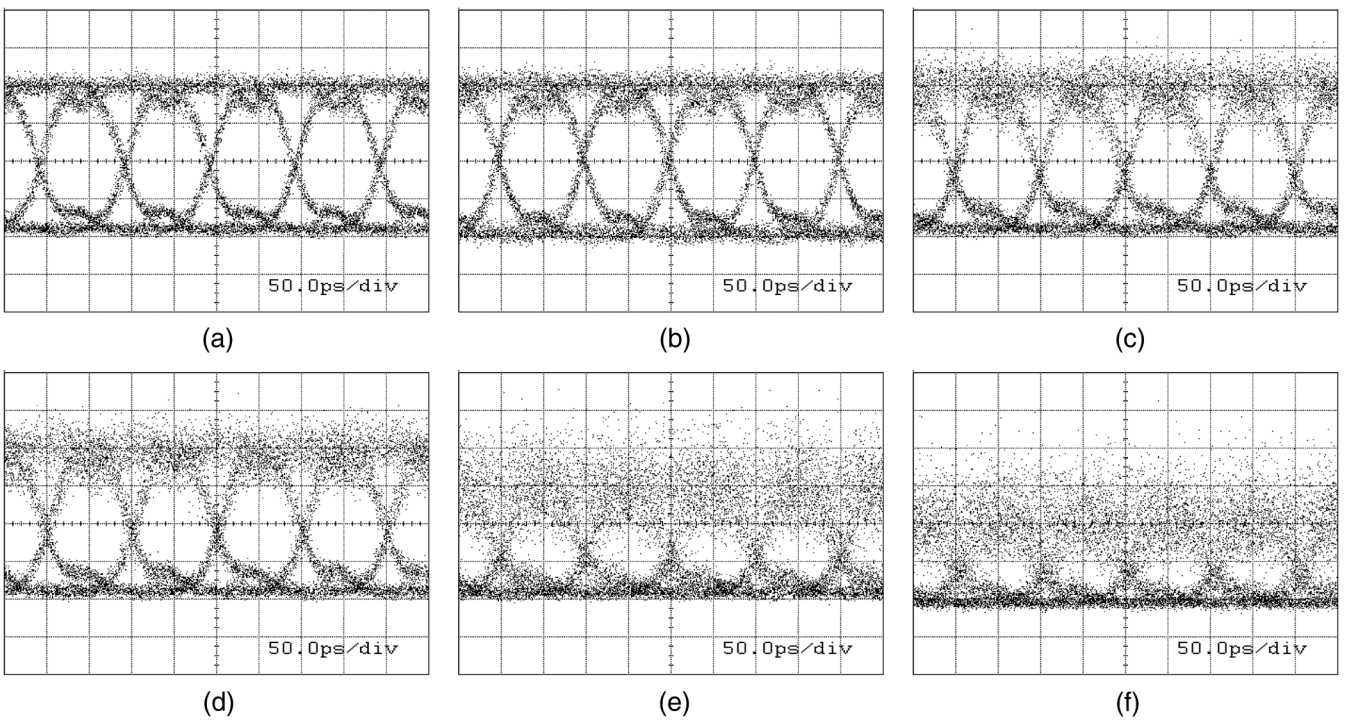

Fig. 8 Eye diagrams of a 1 × 6 broadcast at different wavelengths with channel interval of 100 GHz: (a) at 1555.2 nm (λ_1), (b) 1557.6 nm (λ_2), (c) 1554.4 nm (λ_3), (d) 1558.4 nm (λ_4), (e) 1553.6 nm (λ_5), and (f) 1559.2 nm (λ_6).

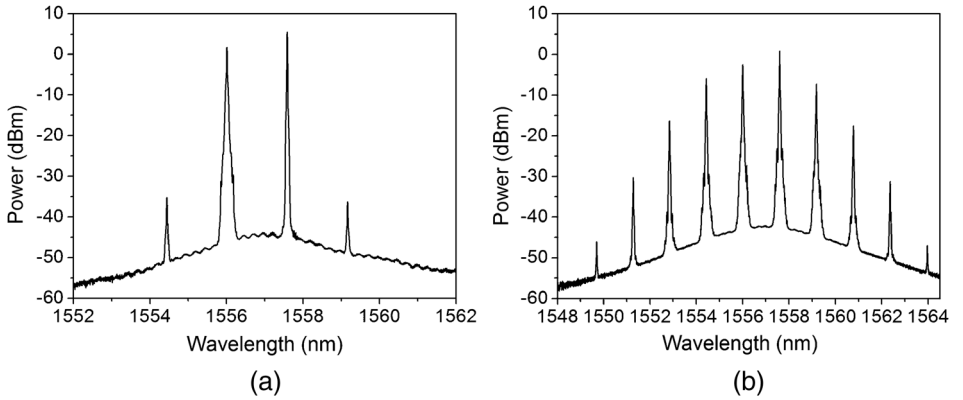

Fig. 10 Optical spectra at the (a) input and (b) output of the AL-HNLF with a channel interval of 200 GHz.

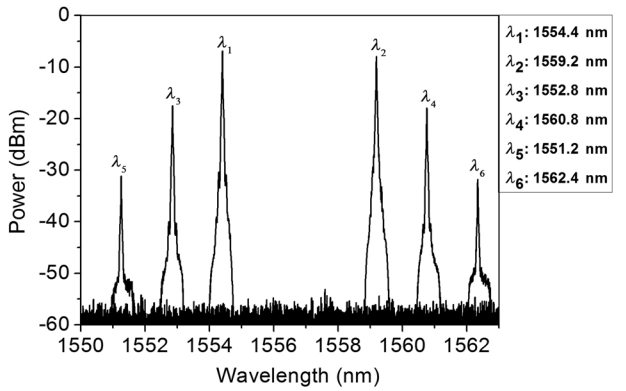

Fig. 11 Optical spectra of the broadcast signals after the filtering subsystem (channel space: 200 GHz).

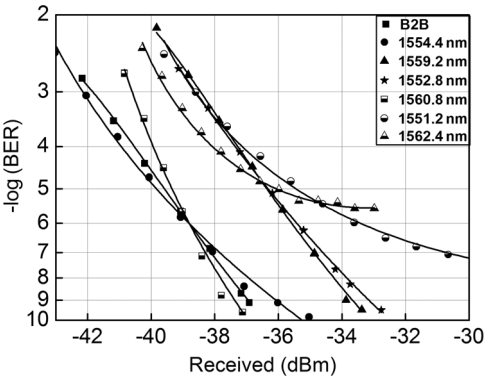

Fig. 13 BER curves of the six broadcast signals (channel space: 200 GHz).

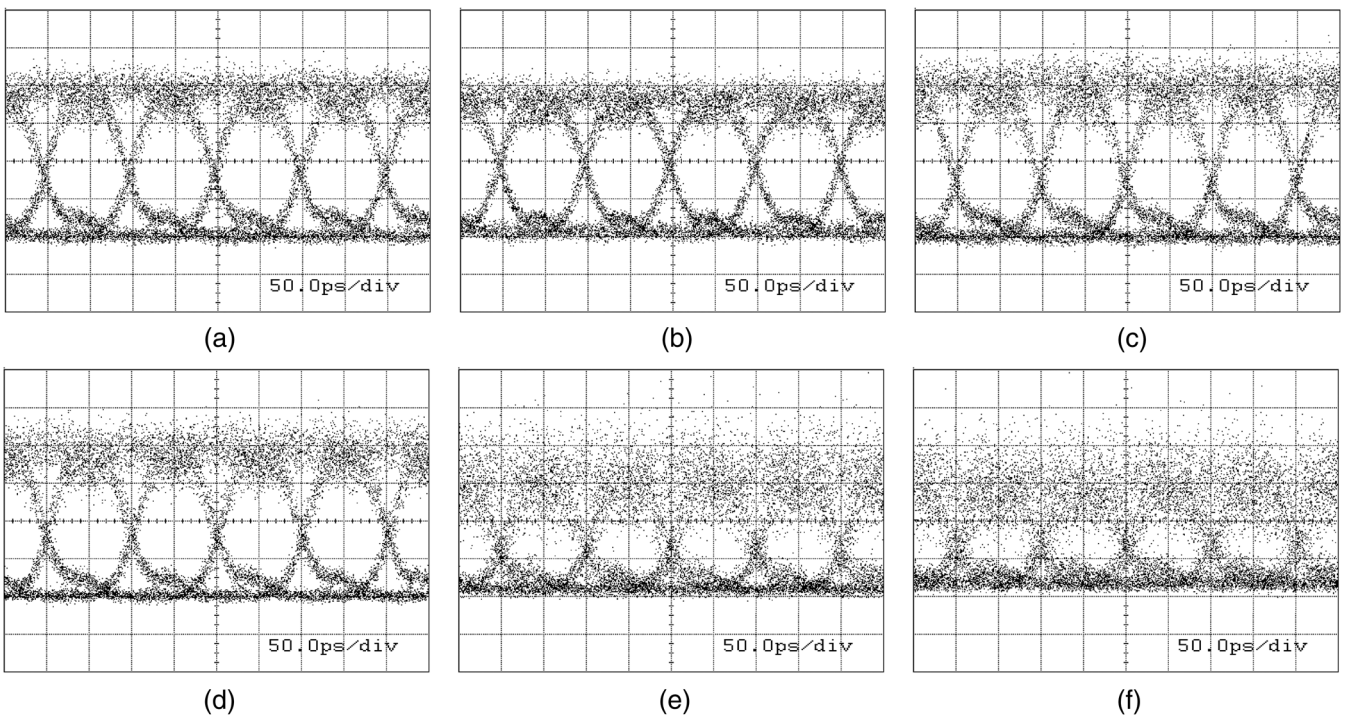

Fig. 12 Eye diagrams of a 1×6 broadcast at different wavelengths with channel interval of 200 GHz: (a) at 1554.4 nm (λ_1), (b) at 1559.2 nm (λ_2), (c) at 1552.8 nm (λ_3), (d) at 1560.8 nm (λ_4), (e) at 1551.2 nm (λ_5), and (f) at 1562.4 nm (λ_6).

depict the optical spectra and eye diagrams at different wavelengths for the new generated signals. The analysis is similar to 50 GHz. The BERs of broadcast signals are shown in Fig. 13. The case is similar to 50 GHz.

4 Conclusion

In this paper, three different channel intervals of 50, 100, and 200 GHz broadcast experiments have been implemented, respectively. The clear eye diagrams as well as the low error performance demonstrate the broadcast technology based on AL-HNLF without any SBS suppression stage. Although data signals at λ_1 and λ_6 are not as good as the others, they can still be improved by reducing coupling losses and losses in the AL-HNLF or increasing the magnification of the EDFA. Additionally, though these experiments are conducted at 10 Gb/s and since FWM possesses the transparent characteristics of fast response and signal processing in data format, similar results can be extracted at other rates. Consequently, these three experiments show that the wavelength is tunable, which indicates a strong application for broadcast technology.

Acknowledgments

The authors would like to thank Professor Enze Yang and Professor Jinlong Yu at the School of Electrical and Information Engineering in Tianjin University and thank Ju Wang for the support in the experiments.

References

1. Q. Huang and W.-D. Zhong, "Wavelength-routed optical multicast packet switch with improved performance," *J. Lightwave Technol.* **27**(24), 5657–5664 (2009).
2. Q. Huang and W.-D. Zhong, "An optical wavelength-routed multicast packet switch based on multitimeslot multiwavelength conversion," *IEEE Photonics Technol. Lett.* **20**(18), 1518–1520 (2008).
3. M. Ahlawat et al., "Tunable single-to-dual channel wavelength conversion in an ultra-wideband SC-PPLN," *Opt. Express* **21**(23), 28809–28816 (2013).
4. L. Liu et al., "Experimental demonstration of RSOA-based WDM PON with PPM-encoded downstream signals," *Chin. Opt. Lett.* **10**, 070608 (2012).
5. C. L. Wu, S. P. Su, and G. R. Lin, "All-optical data inverter based on free-carrier absorption induced cross-gain modulation in Si quantum dot doped SiOx waveguide," *IEEE J. Sel. Top. Quantum Electron.* **20**(4), 8200909 (2014).
6. X. Jin, T. Keating, and S. L. Chuang, "Theory and experiment of high-speed cross-gain modulation in semiconductor lasers," *IEEE J. Quantum Electron.* **36**(12), 1485–1493 (2000).
7. G. Contestabile et al., "Cross-gain modulation in quantum-dot SOA at 1550 nm," *IEEE J. Quantum Electron.* **46**(12), 1696–1703 (2010).
8. C. Meuer et al., "Cross-gain modulation and four-wave mixing for wavelength conversion in undoped and p-doped 1.3-μm quantum dot semiconductor optical amplifier," *IEEE J. Photonics* **2**(2), 141–151 (2010).
9. M. Usami et al., "Experimental analysis of cross gain modulation and cross phase modulation in SOA with assist light injection," in *All-Optical Networking: Existing and Emerging Architecture and Applications/Dynamic Enablers of Next-Generation Optical Communications Systems/Fast Optical Processing in Optical Transmission/VCSEL*, pp. TuK1-21–TuK1–22 (2002).
10. A. Kapsalis et al., "Tunable wavelength conversion using cross-gain modulation in a vertically coupled microring laser," *IEEE Photonics Technol. Lett.* **21**(21), 1618–1620 (2009).
11. D. Marcuse, A. R. Chraplyvy, and R. W. Tkach, "Dependence of cross-phase modulation on channel number in fiber WDM systems," *J. Lightwave Technol.* **12**(5), 885–890 (1994).
12. J. Y. Yang et al., "All-optical chromatic dispersion monitoring for phase-modulated signals utilizing cross-phase modulation in a highly nonlinear fiber," *IEEE Photonics Technol. Lett.* **20**(19), 1642–1644 (2008).
13. A. Matsumoto et al., "Operational design on high-speed semiconductor optical amplifier with assist light for application to wavelength converters using cross-phase modulation," *IEEE J. Quantum Electron.* **42**(3), 313–323 (2006).
14. G. Contestabile, M. Presi, and E. Ciaramella, "Multiple wavelength conversion for WDM multicasting by FWM in an SOA," *IEEE Photonics Technol. Lett.* **16**, 1775 (2004).
15. Q. Hao and H. Zeng, "Cascaded four-wave mixing in nonlinear Yb-doped fiber amplifiers," *IEEE J. Sel. Top. Quantum Electron.* **20**(5), 1–5 (2014).
16. D. F. Geraghty et al., "Wavelength conversion for WDM communication systems using four-wave mixing in semiconductor optical amplifiers," *IEEE J. Sel. Top. Quantum Electron.* **3**(5), 1146–1155 (1997).
17. R. Su et al., "Proposal of interaction length for stimulated Brillouin scattering threshold of nanosecond laser in optical fiber." *Opt. Laser Technol.* **57**, 1–4 (2014).
18. R. Su et al., "Numerical analysis on impact of temporal characteristics on stimulated Brillouin scattering threshold for nanosecond laser in an optical fiber," *Opt. Commun.* **316**, 86–90 (2014).
19. T. Nakanishi et al., "Al_2O_3-SiO_2 core highly nonlinear dispersion-shifted fiber with Brillouin gain suppression improved by 6.1 dB," in *32nd European Conf. on Optical Communication (ECOC) 2006*, Th4.1.2 (2006).

Lijuan Li is a graduate student at Tianjin University. She received her BS degree in communication engineering from Tianjin University in 2012. Her current research interests include optical application and sensors.

Jinlong Yu received his MS and PhD degrees from Tianjin University, China, in 1994 and 1997, respectively. In 1997, he joined Tianjin University. He became a full professor and group leader in the Optical Fiber Communication Laboratory of Tianjin University. He researches high-speed optical signal processing and functional elements for radio over fiber and RoF applications.

Ju Wang received her BS and MS degrees from Tianjin University in 2008 and 2010, respectively, and her PhD degree from Tianjin University in 2013. Her doctoral work principally concerned optical signal processing, especially all-optical regeneration in highly nonlinear fiber. In 2012, she joined the High-Speed Optical Communications Group at the Technical University of Denmark as a visiting PhD student. Since September 2012, she has been working with the Optical Fiber Communication Laboratory of Tianjin University. Her research interests include all-optical signal processing and optoelectrical oscillators.

Wenrui Wang is an associate professor at Tianjin University and his research interests include optical fiber communication and photonic microwaves.

Shi Jia is a PhD student at Tianjin University.

Qiong Wu is a graduate student at Tianjin University whose current research interests include optical application and sensors.

Lixia Dou is a graduate student at Tianjin University whose current research interests include optical application and sensors.

Biao Huang is a graduate student at Tianjin University whose current research interests include optical application and sensors.